CAPABILITY OF LOAD-TIME HISTORY RECONSTRUCTION AND FATIGUE CRACK GROWTH RATE ESTIMATION FOR 2024-T3 ALUMINIUM ALLOY ON THE BASIS OF FRACTOGRAPHIC ANALYSIS

D. Kocańda , J. Torzewski

Military University of Technology , Warsaw, Poland

Abstract. The subject of the paper is the considerations of the capability of load-time history reconstruction for the component under variable amplitude loading and fatigue crack growth rate estimation for the 2024-T3 Alclad aluminium alloy on the basis of microfracture analysis. For this goal three variable amplitude (VA) load sequences with multiple overloads and differing from the level of load sequence complexity were applied. These loads are employed when simulating the fatigue behaviour of aeronautical alloys. To reveal the load sequence effect on crack growth behaviour the microfracture analysis were provided by means of TEM microscope.

Introduction

Fractographic analysis is practically used since many years in order to analyse the failure case of real structures and to reconstruct the exploitative loading of failed components. The importance of fractography supporting those analyses was pointed out in the books published either by V.C Ivanova et al. [1] or by J. Schijve [2]. However, in many cases either of the loads or the tested materials, the fatigue striations may be invisible on the fracture surface and the load reconstruction impossible. This case is often observed in aluminium alloys. On the other side special needs concerning fatigue damage of aircraft components inspire the researchers to investigate fatigue crack propagation in aerospace aluminium alloys under different types of loading to learn the striation systems formed on the fracture surface. For load histories containing overloads, the evidence of fatigue striations on fracture surface depends on particular combination of load parameters and material. It can happen that the multiple overloads which intersperse the baseline cycles do not mark the striations on the fracture surface. A negligible effect of overloads on the crack growth rate appeared in aluminium alloys such as 2024-T3 [3], 7075 and 8090 [4] under aircraft service spectrum as well as in another seven aerospace aluminium alloys [5]. This fact was confirmed by the plots of crack growth rate also for 2524-T3 Alclad aluminium sheets under the Embraer simulated service utilisation. To the contrary, stronger interaction effects on crack growth behaviour appeared in 2024-T3 when a single overload was applied and consequently multiplied until failure [3]. The mentioned results were also confirmed in our research developed for 2024-T3 aluminium alloy [6].

The present work derives the results of fatigue crack growth response in 2024-T3 Alclad aluminium alloy to the application of three variable amplitude (VA) load sequences which are employed when simulating the fatigue behaviour of aeronautical alloys. The problem of reconstruction of the load-time history of the component as well as the fatigue crack growth rate estimation on the basis of microfracture analysis is also considered here.

Material. Experimental procedure

The material used for testing was 2024-T3 Alclad aluminium alloy sheet of 3 mm thickness. Clad layer thickness was 0.120 mm. The central crack tension specimens (CCT) had the size of 400 mm length and 100 mm width. In order to facilitate comparison of fatigue properties with respect to sheet rolling direction, the specimens were cut in directions parallel (LT) and transverse (TL) due to rolling. The mechanical properties were in the following ranges: ultimate tensile stress 447-466 MPa, yield stress 303-335 MPa, elongation 21-24%. The highest values of these properties were found for LT specimens. The average grain diameters in the clad layer were 85-89 μm, and in the matrix material, respectively, 29-35 μm in the LT direction and 18-25 μm in TL one. In those specimens tested under constant

amplitude (CA) cyclic tension (R=0.1) the crack growth rates were found to be independent on the cutting direction.

For crack propagation studies, the specimens were provided with a central notch consisting of a through-thickness hole of 5 mm diameter, through-thickness saw cut of 2,5 mm length and pre-cracking of 2.5 mm length on each side of the hole. The initial crack length was equalled to $2l$=15 mm, counting the length from tip to tip of pre-cracking. All fatigue tests were carried out under load control cyclic tension with a frequency of 2 Hz.

To check the ability of microfracture analysis for the load-time history reconstruction for 2024-T3 aluminium alloy three variable amplitude (VA) load programs (Figs. 1, 2a and 2b) were applied that differ from the level of load sequence complexity. They are employed for crack propagation tests under flight simulation loads of lower skin of aircraft wing. First program named here as OVL was proposed by J. Schijve. It contains a load sequence of 211 cycles with few overloads, as shown in Fig. 1. The basic constant-amplitude load (CA) is interspersed by 10 uploads, and then by a single similar upload followed by 100 basic cycles. Successive 10 overloads are also preceded by 100 basic cycles. Maximum stress at the overload is S_{max}= 100 MPa, the overload rate OLR=1.266. Overload rate OLR is defined as $OLR=(K_{OL}-K_{min,\,BL})/(\Delta K_{BL})$, where K_{OL}, $K_{min,BL}$ and ΔK_{BL} mean stress intensity factors at the overload and at the minimum stress of basic cycles and the range of stress intensity factor calculated for the baseline, respectively. Second load program called as LHL-100 (Fig. 2a) has a flight schedule of 100 flights with the load cycles ordered in 13 blocks.

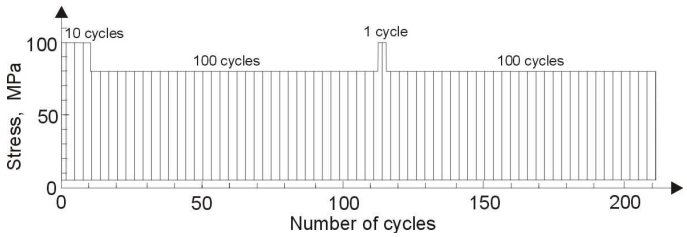

Fig.1. Load sequence with overloads (OVL-program)

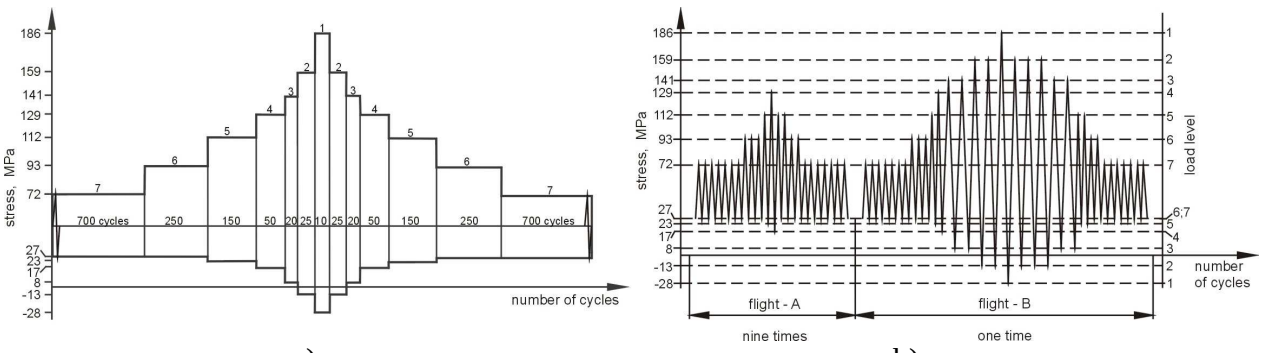

a) b)

Fig. 2. Scheme of LHL-100 block program (a) and FAF cycles sequence (b)

Each block has the same maximum and minimum load, but the range of the stress amplitude and the number of cycles depend on the stress levels numbered from 1 to 7. One LHL-100 program has 2400 total number of cycles. Third VA load program called as FAF (flight-after-flight), with the scheme shown in Fig. 2b, consists of two blocks of cycles: Flight A and Flight B. Within one FAF load sequence the block Flight A is nine times repeated whereas block Flight B only one time. One load sequence counts 240 cycles. Either Flight A or Flight B are of the low-high-low shape with various magnitude spike overloads-underloads. Ten FAF sequences equilibrate one LHL-100 block program. All load programs were repeated until the specimen failure. The X-ray diffraction method revealed the compressive residual stresses of value 40 MPa in the Alclad layer either in pre-cracked or

without pre-cracked LT and TL specimens.

The crack length was monitored visually using a magnifying glass. For visual recording of the crack tip positions a line scale was inscribed on the specimen surfaces along the crack path. The accuracy of crack length readings was 0.2 mm.

Additionally, the region of the crack tip was recorded by the video camera. The load sequence effect on crack growth rate behaviour was analysed by means of the transmission (TEM) electron microscope. Prior to the TEM observations the plastic replicas taken from the fracture surfaces were shadowed by platinum.

Results and discussion

Fatigue crack growth under variable amplitude loading. It should be emphasized that the considerations for fatigue crack growth behaviour under variable amplitude loading (VA) refer only to long crack. The discussion of the obtained results will be provided separately for each load test.

Test results for OVL program

Fatigue crack growth response for 2024-T3 aluminium alloy under OVL program (Fig. 1) is analysed on the basis of Fig. 3 and Fig. 5 as well as the image in Fig. 4 of the fracture surface with fatigue striations relevant to this load program. In Fig. 3 experimental data set of the surface crack growth rates referred to OVL program was compared with the data associated with surface crack growth rate under CA loading. As it was expected, the multiple overloads imposed in the stress amplitude baseline caused a significant reduction in growth rates. However, the retardation and acceleration effects associated with a particular block of overloads are not clearly visible on the experimental plots in Fig. 3. On the contrary, the effects of the overloads on crack growth rate can be considered when taking into account the TEM micrograph that originates from the spots at different distances from the notch root. Exemplary TEM micrograph with the striations seen in Fig. 4 corresponds to a half of the load sequence. On the image, from left to the right side, one can easily identify the band with 10 „thicker" striations attributed to 10 applied overloads, then the band with 100 „tiny" striations corresponded to 100 basic cycles and a single "thicker" striation induced by one overload. Ten overloads give rise to severe retardation effect which appears immediate after applying the overloads. When approaching the single thicker striation then the spacing between them gradually increases because of an acceleration in growth rate.

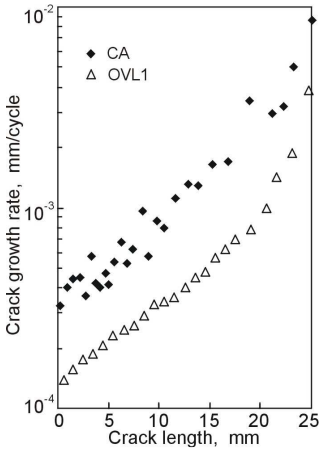

Fig. 3. Courses of crack growth rates versus crack length under CA and OVL load program

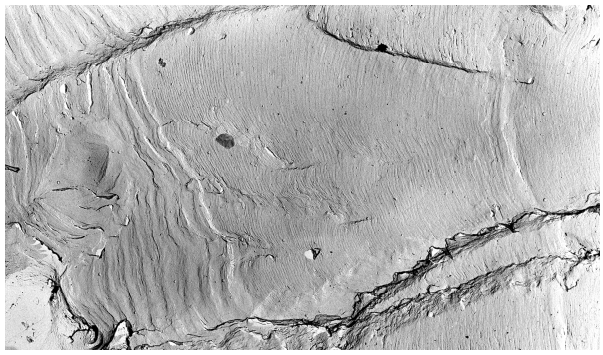

Fig. 4. TEM micrograph illustrates the system of fatigue striations formed under OVL load test

The TEM micrograph allow us accurately reconstruct the history of loading as well as the changes of crack growth rates in 2024-T3 alloy under the OVL loading.

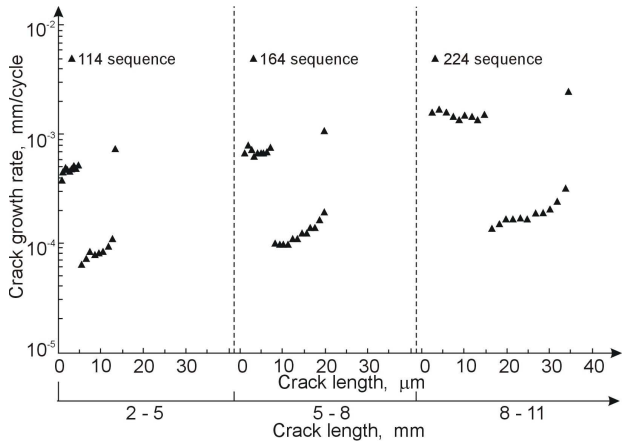

Fig.5. Courses of local crack growth rate against crack length; see text for explanation

The courses of local growth rates affected by particular whole cycle sequences and estimated on the basis of striations spacing against crack length are shown in Fig 5. On double horizontal axis are marked the intervals of the crack length increment in millimetres, counting from the pre-cracking, whereas on the lower axis the crack length increment in micrometers is calculated from the striations spacing. As it is seen on the diagram ten overloads produce initially a high growth rate. However, under successively following overloads in the sequence the rate shows a decreasing tendency and eventually a rapid drop almost of two orders of magnitude. Afterwards, the rate gradually increases in the period corresponded to 100 baseline cycles showing also certain periods of constant rates. Imposition of a single overload in the basic cycles results either in an immediate short jump of growth rate or its rapid drop of one order of magnitude. The load interaction leads to a delayed retardation of crack growth and then to its gradual rising in the period associated with the application of subsequent 100 basic cycles. The crack retardation is associated with a plastic zone ahead of a crack tip, produced by the overloads. The compressive stresses acted in this zone temporarily close the tip of the crack. As it is seen in the diagram multiple overloads give rise to a more severe crack growth rate retardation than a single overload. One can note a significant rise of crack growth rate with increasing number of load sequences passed in the test.

Test results for LHL-100 block program loading

Results of fatigue crack growth rates relevant to the LHL-100 loading as well as to the CA test against measured surface crack length are shown in Fig. 6 for two LT specimens.

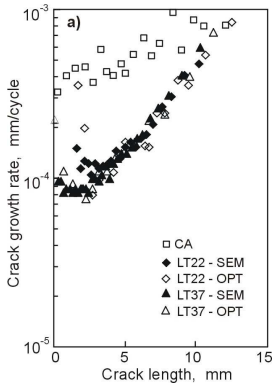

Fig. 6. Comparison of crack growth rates for LHL-100 block program and CA loading against crack length

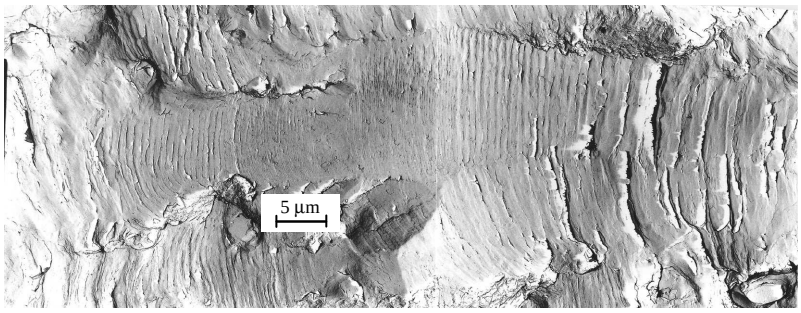

Fig. 7. TEM micrograph with the systems of fatigue striations relevant to LHL-100 block program

The data marked by open (white) symbols refer to the crack length recorded visually (OPT). The data marked by filled-in black symbols represent fractographic measure (SEM) of crack depth by using SEM microscope. Discrepancies between these two VA data sets are small.

Similar trend was observed for TL specimens, though crack growth rate was slightly higher in the TL than in LT specimens. All VA results fall significantly below the CA test

data because LHL block program strongly reduces the growth rate in the most part of the specimens' lifetimes. In the final part of fatigue life the VA growth rate reaches the CA rate. The effect of load interaction on crack growth rates attributed to the particular load blocks is not clearly visible on the experimental plots. To learn better this effect the TEM micrographs should be analysed. Exemplary TEM micrograph in Fig. 7 shows a system of fatigue striations which corresponds to descending and then to ascending parts of one full block program observed on the fracture surface in the distance from 8 to 11 mm from the notch root.

Closer insight into striation systems seen on the micrograph allow linking with the suitable load block and determination of the local crack growth rates cycle by cycle from the striations spacing. The courses of local growth rates attributed to the particular stress levels either in descending or in ascending part of LHL-100 program against crack length are shown in Fig. 8 for three distances from the notch root (pre-cracking). As before, on double horizontal axis are marked the intervals of the surface crack length in millimetres, counting from the pre-cracking, whereas on the lower axis the crack length increment in micrometers is calculated from the striations spacing.

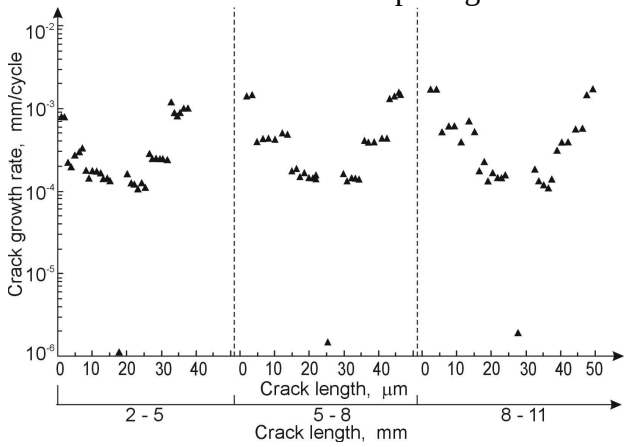

Fig.8. Courses of local crack growth rate against crack length; see text for explanation

As it is seen first level block with ten spike overloads-underloads strongly reduces the growth rates in all blocks. It confirms also the importance of first cycle in each block in producing highest crack increment. The successive cycles in the block change in a small range only the striations spacing. It means the growth rate was almost constant within the block. It should be emphasized that the correlation between the striation systems and the appropriate load blocks was possible for establishing only for the stress levels labelled from 1 to 4 in descending part and respectively for 4-1 levels in the ascending part of the LHL-100 program.

When following the blocks labelled from 5 to 7 (2300 cycles together) the crack growth rate drops to minimum value of 10^{-6} mm/cycle or even below it and the crack is arrested. This effect is more pronounced for first applied load program. In result the possible crack arrest lasts for 2300 cycles per 2400 all cycles relevant to one LHL-100 program. It suits almost 95.5% of the LHL-100 program duration. On the contrary the propagation period coveres only 100 cycles which states 4.5% of the time of load program affectation. The behaviour of crack growth rate under LHL block program is strongly depended on the plastic induced crack closure as well as the changes of stress distribution at the crack tip.

Test results for FAF load program

The FAF load program (Fig. 2b) has a common derivation with the LHL-100 block program but differs from this latter the ordering and the number of cycles in the particular blocks. The FAF sequence includes only one spike overload-underload of highest stress ratio S_{UNmin}/S_{OVmax}= -0.15. The interaction of this loading on the crack growth behaviour one can learn considering the experimental results performed in the figs 9 and 11 as well as the TEM micrograph in Fig. 10. To perform the load test results the courses of crack growth rates against visually measured surface crack length for two LT specimens were compared with the result derived by the CA test (Fig. 9).

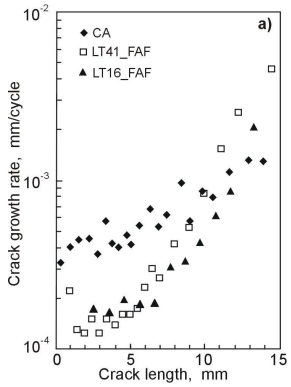

Fig. 9. Comparison of crack growth rate under FAF sequence and under CA against measured crack length

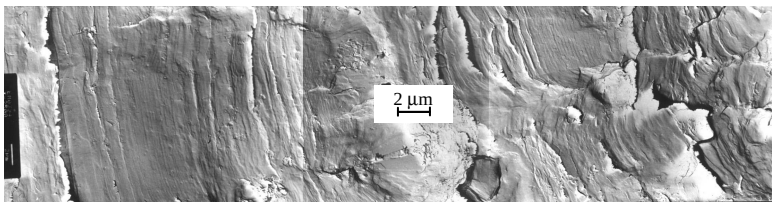

Fig. 10. TEM micrograph with fatigue striations on the fracture surface attributed to FAF load program

It might be expected that the growth rates under FAF loading were bellow the CA data. However, more details of the load influence on the crack growth behaviour derived the TEM micrographs. Exemplary TEM micrograph attributed to the FAF loading presents Fig. 10. The changes of the local crack growth rate within one sequence was estimated cycle by cycle on the basis of the TEM measurements taken from different spots on the fracture surface. The data points shown in Fig. 11 indicate that the highest spike overload and underload cycle of the first stress level plays an important role in the sequence producing a widest striation. On the other side underloading reduces the effect of crack retardation. In the case of FAF loading the crack propagation period covers only 22 cycles per 240 cycles that belong to the whole sequence. In the micro scale crack growth rate attributed to one spike overload-underload cycle is almost three times higher than this one resulted from the action of ten immediately following spike overload-underload cycles in the LHL-100 program.

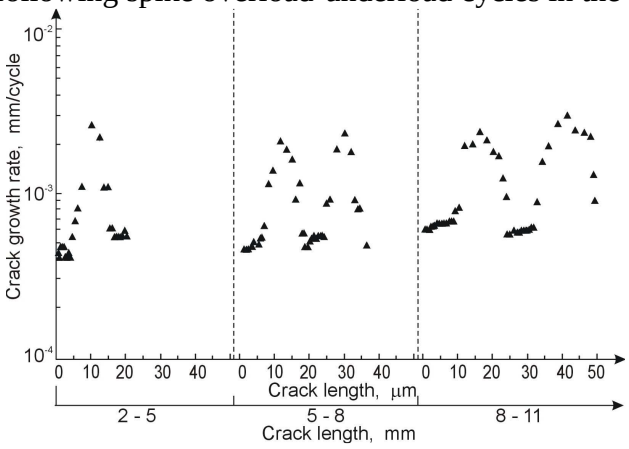

Fig. 11. Courses of local crack growth rate against crack length; see text for explanation

Finally, the lifetimes of the specimens tested under the FAF loading are lower than those ones under the LHL-100 block program. In the case of a complex VA load sequences with a certain number of immediately following spike overloads-underloads the reconstruction of the load-time history on the basis of microfracture analysis is limited. The TEM observations allow identifying only a part striations attributed to the particular cycles in the load sequence. This limited reconstruction results also from short return period load programs considered here.

Our research developed in this field indicate that in the case of simple load programs with block of spike overloads-underloads with longer return periods the correlation between the fatigue striations and the relevant load cycles is very good in whole range of crack length.

Conclusions

The study for 2024-T3 aluminium alloy sheet was undertaken in order to learn about the influence of variable amplitude loading with multiple spike overloads-underloads on fatigue crack growth behaviour and to recognise the ability of load-time history reconstruction. Three load sequences were considered here, namely simple OVL load program, the FAF (flight-

after-flight) cycles sequence and LHL-100 block program that differed from the ordering and the number of various magnitude overloads-underloads. The results indicate very important role played by first overload-underload cycle in the sequence of either the FAF or the LHL-100 loads.

The research proves as well that a short return period occurred in the load program with a certain number of immediately following spike overload-underload cycles introduces the limitation for the reconstruction of the load-time history on the basis of microfracture analysis.

References

1. Ivanova V., Shaniavsky A. Quantitative fractography. Metallurgy Press, 1988 (in Russian).
2. Schijve J.: Fatigue of Structures and Materials. Kluwer Academic Publishers, 2001.
3. Kermanidis A.T., Pantelakis S.G. Fatigue crack growth analysis of 2024-T3 aluminium specimens under aircraft service spectra. Fatigue Fract. Engng Mater. Struct., 2001, Vol. 24, p. 699-710.
4. Ranganathan N. Certain aspects of variable amplitude fatigue. Proc. Eighth Int. Fatigue Congress Fatigue 2002, Sweden, Ed.: A. Blom, Vol. 1/5, pp. 613-621, 2002.
5. Brockenbrough J.R., et al. Crack growth prediction methods for spectrum loading to support fatigue and durability damage tolerance evaluation. ICAF 2003, Switzerland, 2003, p. 14.
6. Kocańda D., Kocańda S., Torzewski J. Reconstruction of fatigue crack growth rate for 2024-T3 aluminium alloy sheet on the basis of fractographic analysis. Archive Mech. Engng, Vol. LI, No 3, pp. 361-376, 2004.